Transport of a nonneutral electron plasma due to electron collisions with neutral atoms

M. H. Douglas and T. M. O'Neil

Department of Physics, University of California, San Diego, La Jolla, California 92093
(Received 16 September 1977; final manuscript received 13 February 1978)

Transport of a nonneutral electron plasma across a magnetic field is caused by electron scattering from ambient neutral atoms. A theoretical model of such transport is presented, assuming the plasma is quiescent and the scattering is elastic scattering from infinite mass scattering centers of constant momentum transfer cross section. This model is motivated by recent experiments. A reduced transport equation is obtained by expanding the Boltzmann equation for the electron distribution in inverse powers of the magnetic field. The equation together with Poisson's equation for the radial electric field, which must exist in a nonneutral column, determine the evolution of the system. When these two equations are properly scaled, they contain only a single parameter: the ratio of initial Debye length to initial column radius. For cases where this parameter is either large or small, analytical solutions, or at least partial solutions, are obtained. For intermediate values of the parameter, numerical solutions are obtained.

I. INTRODUCTION

The transport of a nonneutral electron plasma across a magnetic field has been studied in recent experiments.[1] The experiments show that the transport time scales inversely with the pressure of the ambient gas. The simplest model consistent with this observation assumes that the transport is classical and results from electron-neutral collisions in a quiescent plasma. We provide a theoretical description of such transport.

The plasma in the experiments[1] is in the shape of a cylindrical column with a cylindrical absorbing wall as its outside boundary. Confinement in the radial direction is provided by a large axial magnetic field, and confinement at the ends is provided by cylinders, or similar structures, biased negatively relative to the walls. For our model, we assume perfect cylindrical symmetry and infinite length. The ambient gas in the experiment may be varied.[1] For the case of helium, the electron kinetic energy remains below the lowest excited state of the atom. With this case in mind, we assume the electrons scatter elastically off stationary infinite mass scattering centers. An electron does not make enough collisions during the course of an experiment for corrections due to the finite mass of the helium to be important. Since the momentum transfer cross section for electron-helium collisions is nearly independent of energy in the relevant energy range, we treat it as a constant.[2] Also, the electron-electron collision time is longer than the duration of the experiment, so we neglect these collisions.

Our model, then, assumes a quiescent, cylindrical, infinitely long, electron column immersed in a large axial magnetic field, with the electrons scattering elastically off stationary infinite mass scatterers. The part of this model which is most likely to be in serious conflict with the experimental is the assumption that the plasma is quiescent. There is evidence[3] that in a certain parameter range the transport is anomalous. Nevertheless, it seems worthwhile to calculate the classical transport as a benchmark in any case. Also, the physics of the quiescent transport is interesting and rather unusual, and it is that physics we wish to discuss here.

In general, electron neutral transport cannot be described adequately in terms of coupled fluid equations for the electron density and temperature profiles.[4,5] The electron distribution becomes non-Maxwellian and a description in terms of the Boltzmann equation is required. When an electron scatters elastically from a stationary infinite mass scatterer, there is no change in the electron kinetic energy. The collisions cannot redistribute electron kinetic energy and make the distribution Maxwellian; of course, the collisions do make the distribution directionally isotropic.

Although a description in terms of the Boltzmann equation is necessary, one need not keep all of the information content in that equation. For example, the phase of an electron in its gyromotion around the magnetic field is unimportant, for a large enough field. In Sec. II, we expand the Boltzmann equation in inverse powers of the field and obtain a reduced transport equation for the lowest order, or phase averaged, part of the distribution. The magnetic field in the experiment of Ref. 1 is large enough to justify the expansion.

The reduced transport equation obtained here is related to that used to describe the evolution of the electron distribution in a partially ionized gas, or swarm.[4,5] For example, the reduced transport equation obtained by Bernstein[5] reduces to ours when his is specialized to the large magnetic field limit. However, his derivation is based on an expansion in large collision frequency, rather than large magnetic field, or large gyrofrequency. Probably the most important difference between our work and the work on partially ionized gases lies in our treatment of the electric field, which appears as a driving term in the reduced transport equation. For a nonneutral plasma the radial electric field is produced by the electrons themselves and is self-consistently related to the distribution through Poisson's equation. We solve the reduced transport equation simultaneously with Poisson's equation.

In Sec. III, the reduced transport equation and Poisson's equation are scaled and solutions are obtained. The scaled equations contain only a single parameter: the

 0031-9171/78/2106-0920$00.90

ratio of initial Debye length to initial column radius. When this ratio is large, the radial electric field is unimportant and diffusion dominates the transport. Since collisions do not change the energy of an electron, the diffusion occurs separately for each energy class, and the higher energy (i.e., faster) electrons diffuse out of the column first; this is called diffusion cooling (Ref. 4, p. 75). An analytic solution may be obtained in this limit. In the opposite limit of small Debye length, the solution is characterized by rapid Joule heating followed by transport due to mobility and diffusion. The initial heating may be described analytically. In this limit the velocity distribution near the edge of the column ultimately develops into a spherical shell in velocity space. This is what one expects for electrons that have fallen through a potential energy drop large compared with their initial thermal energy. Recall that the electron-neutral collisions do not change the energy of an electron as the electron wanders out.

For arbitrary values of the ratio, the equations are solved numerically. An interesting feature of the numerical solutions concerns the number of particles remaining in the column as a function of time. The inverse of this number is asymptotically proportional to the time t, for arbitrary values of the ratio of Debye length-to-column radius. This should be useful in comparisons with experiment.

II. DERIVATION OF THE REDUCED TRANSPORT EQUATION

In this section, we expand the Boltzmann equation in inverse powers of the magnetic field and obtain a simplified, or reduced transport equation. As spatial variables, we use cylindrical coordinates (r, θ, z). As velocity variables we also use cylindrical coordinates $(v_\perp, \psi, v_z)$, where $(v_x, v_y, v_z) = (v_\perp \cos\psi, v_\perp \sin\psi, v_z)$. The symmetry assumptions in our model imply that the electron distribution is independent of z and that θ and ψ enter only as $\beta = \psi - \theta$. The electron density and electric potential depend only on r, and the electric field is in the r direction. In terms of the variables $(r, \beta, v_\perp, v_z, t)$ the Boltzmann equation can be written as

$$\frac{\partial f}{\partial t} + \cos\beta\left(v_\perp \frac{\partial}{\partial r} - \frac{e}{m} E \frac{\partial}{\partial v_\perp}\right) f - \sin\beta\left(\frac{v_\perp}{r} - \frac{eE}{m v_\perp}\right)\frac{\partial f}{\partial \beta} + \Omega \frac{\partial f}{\partial \beta} = C(f) \ , \tag{1}$$

where $\Omega = eB/mc$. For elastic collisions with stationary infinite mass scatterers, the collision operator takes the form

$$C(f) = n_n v \int d\Omega\, \sigma(\alpha, v)[f(r, v_\perp' v_z', \beta', t) - f(r, v_\perp, v_z, \beta, t)] \ , \tag{2}$$

where n_n is the density of scatterers, $\sigma(\alpha, v)$ is the differential scattering cross section, α is the scattering angle, $v = (v_z^2 + v_\perp^2)^{1/2}$, and $v' = v$. A quantity that will emerge in the derivation that follows is the momentum transfer cross section

$$\sigma_m(v) = 2\pi \int_0^\pi d\alpha \sin\alpha (1 - \cos\alpha)\, \sigma(\alpha, v) \ . \tag{3}$$

Of course, the electric field is related self-consistently to the distribution through Poisson's equation.

The various terms in the Boltzmann equation all have the dimensions of a frequency times the distribution function. In accord with the experiment of Ref. 1, we assume that the largest of these frequencies is Ω and that the others are ordered relative to Ω in the following manner:

$$\frac{1}{\Omega}\frac{v_\perp}{f}\frac{\partial f}{\partial r} \sim O(\epsilon), \quad \frac{eE}{\Omega m}\frac{1}{f}\frac{\partial f}{\partial v_\perp} \sim O(\epsilon) \ , \quad \frac{1}{\Omega}\frac{C(f)}{f} \sim O(\delta) \ , \tag{4}$$

where $\delta \lesssim \epsilon \ll 1$. It may be instructive to rewrite the ordering as r_L/r, $v_d/\bar{v} \sim O(\epsilon)$ and $\nu/\Omega \sim O(\delta)$, where r_L is the Larmor radius, $v_d = cE/B$ is the drift velocity, $\bar{v}$ is the thermal velocity, and ν is the collision frequency. For time dependence due to transport alone (i.e., no waves), the time derivative enters in the order

$$\frac{1}{\Omega}\frac{1}{f}\frac{\partial f}{\partial t} \sim O(\epsilon^2 \delta) \ ; \tag{5}$$

this will emerge from the derivation. By expanding f in a power series in ϵ and δ,

$$f = \sum_{n,m} f_{n,m} \ , \tag{6}$$

where $f_{n,m} \sim O(\epsilon^n \delta^m)$, Eq. (1) generates a series of equations for the various $f_{n,m}$.

In order $\epsilon^0\delta^0$, the equation is

$$\Omega \frac{\partial f_{0,0}}{\partial \beta} = 0 \ , \tag{7}$$

which has the solution $f_{0,0} = f_{0,0}(r, v_z, v_\perp, t)$. In order $\epsilon^0\delta^1$, the equation is

$$\Omega \frac{\partial f_{0,1}}{\partial \beta} = C(f_{0,0}) \ . \tag{8}$$

Since the $f_{n,m}$ are single valued functions of β, the integral of both sides of this equation over a complete cycle in β must be zero. This yields the constraint equation

$$0 = \int_0^{2\pi} d\beta C(f_{0,0}) = 2\pi C(f_{0,0}) \ , \tag{9}$$

which implies that $f_{0,0} = f_{0,0}(r, v, t)$. Then, by Eq. (8), we see that $f_{0,1} = f_{0,1}(r, v_z, v_\perp, t)$. Constraint equations obtained in this manner are characteristic of this type of expansion.[6] They occur in each order, with the reduced transport equation arising from the constraint in order $\epsilon^2\delta$.

In order $\epsilon^1\delta^0$, the equation is

$$\cos\beta\left(v_\perp \frac{\partial}{\partial r} - \frac{e}{m} E \frac{\partial}{\partial v_\perp}\right) f_{0,0} + \Omega \frac{\partial f_{1,0}}{\partial \beta} = 0 \ . \tag{10}$$

The constraint equation here is satisfied automatically, since $\int_0^{2\pi} d\beta \cos\beta = 0$. The solution is

$$f_{1,0} = h_{1,0}(r, v_z, v_\perp, t) - \frac{\sin\beta}{\Omega}\left(v_\perp \frac{\partial}{\partial r} - \frac{e}{m} E \frac{\partial}{\partial v_\perp}\right) f_{0,0} \ , \tag{11}$$

where $h_{1,0}(r, v_z, v_\perp, t)$ is a solution of the homogeneous

equation (i.e., $\partial h_{1,0}/\partial\beta = 0$). Integrating $\mathbf{v}f_{1,0}$ over velocity yields the first-order flux in the θ direction

$$\Gamma^{(1)} = -\hat{\theta}\frac{1}{\Omega}\left(\frac{\partial}{\partial r}\int\frac{v_\perp^2}{2}f_{0,0}d^3\mathbf{v} + \frac{e}{m}E\int f_{0,0}d^3\mathbf{v}\right)$$

$$= \frac{nc}{B^2}\left(\frac{\nabla P}{ne} + \mathbf{E}\right)\times\mathbf{B} \quad . \tag{12}$$

One can check that all terms which are zero order in δ (i.e., $f_{n,0}$) produce a flux limited to the $\hat{\theta}$ direction. For a radial flux, one must go to first order in δ.

In order $\epsilon\delta$, the equation is

$$\cos\beta\left(v_\perp\frac{\partial}{\partial r} - \frac{e}{m}E\frac{\partial}{\partial v_\perp}\right)f_{0,1} + \Omega\frac{\partial f_{1,1}}{\partial\beta} = C(f_{1,0}) \quad , \tag{13}$$

where

$$C(f_{1,0}) = C(h_{1,0}) - C\left[\frac{\sin\beta}{\Omega}\left(v_\perp\frac{\partial}{\partial r} - \frac{e}{m}E\frac{\partial}{\partial v_\perp}\right)f_{0,0}\right]$$

$$= C(h_{1,0}) + \frac{\sin\beta}{\Omega}\sigma_m(v)n_n v v_\perp\left(\frac{\partial}{\partial r} - \frac{e}{m}\frac{E}{v}\frac{\partial}{\partial v}\right)f_{0,0} \quad .$$

Here, $\sigma_m(v)$ is the momentum transfer cross section defined in Eq. (3). Integrating both sides of Eq. (13) with respect to β yields the constraint equation

$$0 = \int_0^{2\pi} d\beta C(h_{1,0}) = 2\pi C(h_{1,0}) \quad , \tag{14}$$

which has the solution $h_{1,0} = h_{1,0}(r, v, t)$. With the constraint equation satisfied, Eq. (14) may be solved for

$$f_{1,1} = h_{1,1}(v_z, v_\perp, r, t) - \frac{\sin\beta}{\Omega}\left(v_\perp\frac{\partial}{\partial r} - \frac{e}{m}E\frac{\partial}{\partial v_\perp}\right)f_{0,1}$$

$$- \frac{\cos\beta}{\Omega^2}\sigma_m(v)n_n v v_\perp\left(\frac{\partial}{\partial r} - \frac{e}{m}\frac{E}{v}\frac{\partial}{\partial v}\right)f_{0,0} \quad . \tag{15}$$

Integrating $\mathbf{v}f_{1,1}$ over velocity yields the lowest-order flux in the r direction

$$\Gamma_r = -\frac{n_n}{\Omega^2}\frac{4\pi}{3}\int_0^\infty dv\, v^5\sigma_m(v)\left(\frac{\partial}{\partial r} - \frac{e}{m}\frac{E}{v}\frac{\partial}{\partial v}\right)f_{0,0} \quad . \tag{16}$$

By noting that Γ_r must satisfy the continuity equation, one can anticipate that $\partial/\partial t$ enters in order $\epsilon^2\delta$.

In order $\epsilon^2\delta$, we need only the constraint equation, that is, the full equation for this order integrated over a complete cycle in β,

$$\frac{\partial f_{0,0}}{\partial t} - \frac{1}{2}\left[v_\perp\frac{1}{r}\frac{\partial}{\partial r}r - \frac{e}{m}E\left(\frac{1}{v_\perp} + \frac{\partial}{\partial v_\perp}\right)\right]\frac{\sigma_m(v)n_n v v_\perp}{\Omega^2}$$

$$\times\left(\frac{\partial}{\partial r} - \frac{e}{m}\frac{E}{v}\frac{\partial}{\partial v}\right)f_{0,0} = C(h_{2,0}) \quad . \tag{17}$$

Integrating over all angles in velocity space removes the collision operator on the right-hand side and yields the reduced transport equation

$$\frac{\partial f_{0,0}}{\partial t} = \frac{n_n}{3\Omega^2}\left[v^3\frac{1}{r}\frac{\partial}{\partial r}r - \frac{e}{m}E\left(4v + v^2\frac{\partial}{\partial v}\right)\right]$$

$$\times\sigma_m(v)\left(\frac{\partial}{\partial r} - \frac{e}{m}E\frac{1}{v}\frac{\partial}{\partial v}\right)f_{0,0} \quad . \tag{18}$$

Of course, E is given by the solution to Poisson's equation

$$E(r) = -4\pi e\int_0^r\frac{dr'}{r}r'\int_0^\infty 4\pi v^2 dv f_{0,0}(r, v, t) \quad . \tag{19}$$

For the boundary condition, we assume that a perfectly absorbing wall exists at $r = R$ and take $f_{0,0}(R, v, t) = 0$.[5]

By integrating Eq. (19) over all velocity and over the volume of the tube, one can check that the rate of decrease of particles in the tube is accounted for by the flux of particles [i.e., Eq. (16)] at the wall. One can also check that the rate of decrease of kinetic and electrostatic energy in the tube is accounted for by the kinetic energy flux at the wall. The kinetic energy flux is obtained by inserting $1/2\ mv^2$ in the integrand of Eq. (16). These conservation relations are useful in monitoring the numerical algorithm.

III. SOLUTION OF THE REDUCED TRANSPORT EQUATION

Since we ultimately solve Eqs. (18) and (19) numerically, it is useful to scale them properly. The solutions to a variety of problems with different physical parameters are thereby related to the same solutions of the scaled equation. For instance, inspection of Eq. (18) reveals that the evolution of systems that differ only in the value of n_n/B^2 is identical to within a scaling of the time. The experimentally observed scaling[1] with neutral pressure (i.e., effectively with n_n) is what led us to consider electron-neutral transport in the first place. Scaling the equations is particularly useful if we treat the momentum transfer cross section as a constant. This is a reasonable approximation for electron-helium collisions in the experimentally relevant energy range.[2] The cross section can then be factored out of the operator on the right-hand side of Eq. (18) and absorbed, along with the factor n_n/B^2, in a scaled time. Some of the parameters which are useful in the scaling enter through the initial conditions. For simplicity, we model the initial distribution by a four-parameter function

$$f_{0,0}(r, v, 0) = n\exp\left(-\frac{r^2}{a^2}\right)\left[1 - \left(\frac{r}{R}\right)^4\right]\frac{\exp(-v^2/\bar{v}^2)}{(2\pi\bar{v}^2)^{3/2}} \quad , \tag{20}$$

where the parameter a measures the initial radius of the column and the factor $[1 - (r/R)^4]$ simply insures that $f = 0$ at the absorbing wall. Except where explicitly mentioned, our results are relatively insensitive to this choice for the functional form of the initial distribution. The scaling is effected by introducing the variables

$$\rho = \frac{r}{a}, \quad \xi = \frac{v}{\bar{v}}, \quad g = \frac{\bar{v}^3 f_{0,0}}{n} \quad ,$$

$$\tau = \frac{t}{\tau_m}, \quad \frac{1}{\tau_m} = \left(\frac{8\sqrt{2}}{3\sqrt{\pi}}\right)\left(\frac{n_n\sigma\bar{v}\omega_p^2}{\Omega^2}\right) \quad , \tag{21}$$

where $\omega_p^2 = 4\pi ne^2/m$ is the square of the plasma frequency. The time τ_m characterizes transport due to mobility in a uniform Maxwellian plasma. This may be checked by setting $f_{0,0} = n\exp[-v^2/2\bar{v}^2]/(2\pi\bar{v}^2)^{3/2}$ and $E = -4\pi mer/2$ in Eq. (16) and then observing that $\partial n/\partial t = -1/r\,\partial/\partial r(r\Gamma_r) = -n/\tau_m$. Note that $1/\tau_m$ can also be written as $1/\tau_m = \nu\omega_p^2/\Omega^2$, where $\nu = (8\sqrt{2}/3\sqrt{\pi})n_n\sigma\bar{v}$ is the momentum

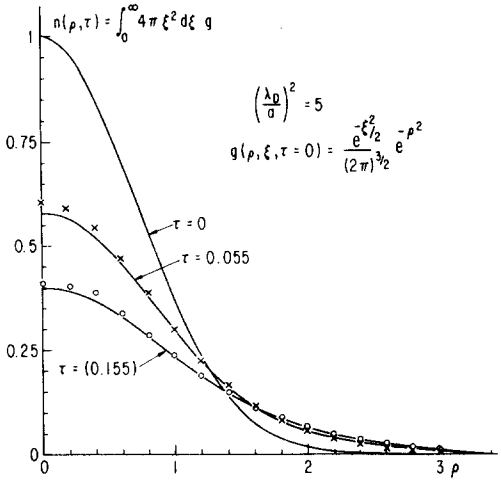

FIG. 1. Evolution of density profile for $(\lambda_D/a)^2 = 5$.

transfer collision frequency. In terms of the scaled variables, Eqs. (18) and (19) can be rewritten as

$$\frac{\partial g}{\partial \tau} = \frac{\sqrt{\pi}}{8\sqrt{2}}\left[\left(\frac{\lambda_D}{a}\right)^2 \xi^3 \frac{1}{\rho}\frac{\partial}{\partial \rho}\rho - \mathcal{E}(\rho,\tau)\left(4\xi + \xi^2\frac{\partial}{\partial \xi}\right)\right] \times\left[\frac{\partial}{\partial \rho} - \left(\frac{a}{\lambda_D}\right)^2 \mathcal{E}(\rho,\tau)\frac{1}{\xi}\frac{\partial}{\partial \xi}\right] g \ , \tag{22}$$

$$\mathcal{E}(\rho,\tau) = -\int_0^\rho \frac{\rho' d\rho'}{\rho}\int_0^\infty 4\pi\xi^2 d\xi\, g(\rho,\xi,\tau) \ , \tag{23}$$

where $\lambda_D^2 = m\bar{v}^2/4\pi ne^2$ is the square of the Debye length. The solutions depend on the parameters λ_D/a and a/R. Typically, a/R is fixed by the experimental geometry, but λ_D/a varies over a large range. Motivated by Ref. 1, we choose $R/a = 3.4$ and study the dependence of the solutions on λ_D/a.

To this end, we multiply out the operator in Eq. (22) and group terms according to the power of λ_D/a they contain. Note that this is equivalent to grouping terms according to the power of $\mathcal{E}$ they contain. There are three types of terms, and they may be associated with the time scales

$$\left(\frac{1}{\tau_d}, \frac{1}{\tau_m}, \frac{1}{\tau_h}\right) = \frac{1}{\tau_m}\left[\left(\frac{\lambda_D}{a}\right)^2, 1, \left(\frac{a}{\lambda_D}\right)^2\right] \ . \tag{24}$$

Here, the time scale τ_m is included explicitly simply to remind us that $\tau = t/\tau_m$ in Eq. (22). We will see that the three time scales are associated with diffusion, mobility, and Joule heating, respectively.

In the limit $\lambda_D/a \gg 1$, τ_d is the shortest time scale. The associated term in Eq. (22) is independent of $\mathcal{E}$ and proportional to the spatial gradients of the distribution. This term produces cross field diffusion on the usual time scale $1/\tau_d = 1/\tau_m(\lambda_D/a)^2 \sim \nu(r_L/a)^2$, where $r_L = \bar{v}/\Omega$. When λ_D/a is large enough, only this term need be retained, and Eq. (22) reduces to

$$\frac{\partial g}{\partial \tau} = \frac{\sqrt{\pi}}{8\sqrt{2}}\left(\frac{\lambda_D}{a}\right)^2 \xi^3 \frac{1}{\rho}\frac{\partial}{\partial \rho}\rho\frac{\partial g}{\partial \rho} \ . \tag{25}$$

The solution of this equation subject to the boundary condition $g = 0$ at $\rho = R/a$ can be written as

$$g(\xi,\rho,\tau) = \frac{e^{-\xi^2/2}}{(2\pi)^{3/2}}\sum_n A_n J_0\left(\rho\frac{a}{R}\chi_{0,n}\right) \times\exp\left[-\xi^3\frac{\sqrt{\pi}}{8\sqrt{2}}\left(\frac{\lambda_D}{a}\right)^2\left(\frac{a}{R}\right)^2\chi_{0,n}^2\tau\right] \ , \tag{26}$$

where $\chi_{0,n}$ is the nth zero of J_0 and the A_n are given by

$$A_n = \frac{\int_0^{R/a} d\rho\,\rho J_0\left(\rho\frac{a}{R}\chi_{0,n}\right) e^{-\rho^2}\left[1-\rho^4\left(\frac{a}{R}\right)^4\right]}{\int_0^{R/a} d\rho\,\rho J_0^2\left(\rho\frac{a}{R}\chi_{0,n}\right)} \ . \tag{27}$$

Later in this section, we obtain a numerical solution of the full equations [i.e., Eqs. (22) and (23)]. Here, we anticipate those results and compare the numerical solution of the full equations to the analytic solution just obtained for the equation with diffusion alone. For the case $(\lambda_D/a)^2 = 5$, Fig. 1 shows the density profile at three successive times; and, for the same three times, Fig. 2 shows the velocity distribution at two radii, $\rho = 0$ and $\rho = 2$. The points are from the analytic solution and the solid curves from the numerical solution. The interesting physics can be seen from the velocity distributions. Near $\xi = 0$, the distributions at both $\rho = 0$ and $\rho = 2$ remain unchanged; whereas, for larger ξ, the distribution at $\rho = 0$ becomes depressed, and the distribution at $\rho = 2$ becomes enhanced. This occurs because the diffusion coefficient is proportional to ξ^3, and the high ξ electrons are the first to diffuse from the center of the column to the outer edges of the column.

For $\lambda_D/a \ll 1$, the time scale τ_h is shortest. The associated term in Eq. (22) is proportional to $\mathcal{E}^2$ and describes Joule heating. Note that $1/\tau_h$ can be rewritten as $1/\tau_h = (1/\tau_m)(a/\lambda_D)^2 \sim eEV_r/m\bar{v}^2$, where $V_r \sim a/\tau_m$ is the radial velocity associated with mobility and we have set $E \sim 4\pi nea$. Although the Joule heating term has the shortest time scale, it does not contribute to electron transport. This can be seen by integrating Eq. (22) over $\xi^2 d\xi$ and noting that the term proportional to $\mathcal{E}^2$ goes out upon integration by parts, that is, it makes no contribution to the radial flux in the continuity equation. The time τ_m characterizes radial transport in the limit $\lambda_D/a \ll 1$. The associated terms in Eq. (22) are proportional to $\mathcal{E}$ and

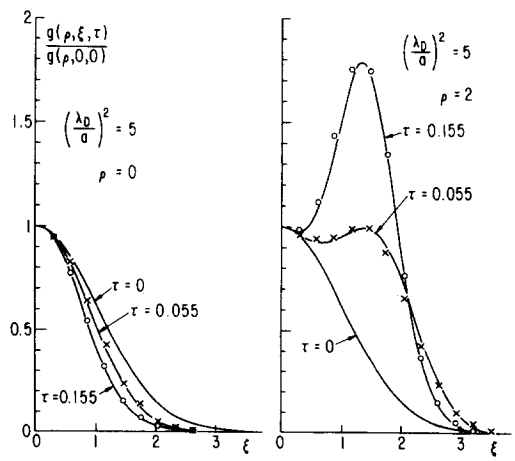

FIG. 2. Evolution of velocity distribution for $(\lambda_D/a)^2 = 5$ and $\rho = 0, 2$.

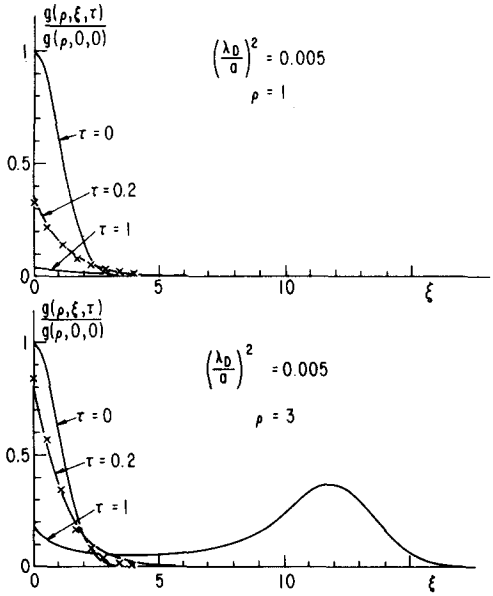

FIG. 3. Evolution of velocity distribution for $(\lambda_D/a)^2 = 0.005$ and $\rho = 1, 3$.

describes the mobility flux. It may seem paradoxical that $\tau_h \ll \tau_m$, since the particles gain energy only by moving out radially. However, τ_h measures the time for a particle to double its energy and τ_m the time for a particle to traverse the column; and, in the limit $\lambda_D/a \ll 1$, a particle can double its energy in moving only a small fraction of the column radius.

To describe the local heating that occurs before transport significantly modifies the spatial distribution, in Eq. (22) we retain only the term associated with τ_h

$$\frac{\partial g}{\partial \tau} = \frac{\sqrt{\pi}}{8\sqrt{2}} \left(\frac{a}{\lambda_D}\right)^2 \mathcal{E}^2 \left(4\xi + \xi^2 \frac{\partial}{\partial \xi}\right)\left(\frac{1}{\xi}\frac{\partial}{\partial \xi}\right) g \quad . \tag{28}$$

Here, $\mathcal{E} = \mathcal{E}(\rho)$ may be evaluated using the initial distribution. As may be checked by direct substitution, the Green's function solution of Eq. (28) is given by

$$g(\rho, \xi, \tau) = \int_0^\infty d\xi' \, 4\pi \xi'^2 g(\rho, \xi', 0)\, G(\xi, \xi', \alpha\tau) \quad , \tag{29}$$

where

$$G[\xi, \xi', \alpha\tau] = \exp\left(-\frac{(\xi + \xi')}{\alpha\tau}\right) I_2\left(\frac{2(\xi\xi')^{1/2}}{\alpha\tau}\right)(4\pi\xi\xi'\,\alpha\tau)^{-1} \tag{30}$$

where I_2 is the Bessel function of imaginary argument, and $\alpha = (\sqrt{\pi}/8\sqrt{2})\,\xi^2(a/\lambda_D)^2$.

A comparison of this solution with the numerical solution of the full equations is shown in Fig. 3, for the case where $(\lambda_D/a)^2 = 0.005$. The upper graph shows the distribution at $\rho = 1$ at three successive times, and the lower graph shows the distribution at $\rho = 3$ at the same three times. The solid curves are from the numerical solution and the points from the analytic solution. One can see that agreement is still good at $\tau = 0.2$. For somewhat later times mobility has caused sufficient transport so that the analytic solution has broken down. We include the numerical solution for $\tau = 1$, to illustrate the distribution after significant transport has occurred. The interesting physics here is the development of the high ξ tails on the distribution. This can also be seen analytically. For sufficiently large $\alpha\tau$, the small argument expansion may be used for I_2 in Eq. (30), and the ξ dependence of the distribution becomes $\exp(-\xi/\alpha\tau)$. After the analytic solution has broken down, the high ξ tail becomes even more pronounced. For example, at $\tau = 1$ and $\rho = 3$, the distribution is nearly a shell in velocity space. Of course, this is what one expects for electrons that move through a potential difference large compared with the initial thermal energy.

To find the solution for arbitrary values of $(\lambda_D/a)^2$, we resort to numerical computation. As a finite difference scheme, we have adapted the method of Dufort and Frankel.[7] This scheme is explicit and stable independent of the magnitude of coefficients of second derivatives; in the reduced transport equation these coefficients can become large because they contain powers of ξ. At this point we could exhibit a series of density profiles and velocity distributions for various times and various values of $(\lambda_D/a)^2$. However, they appear similar to those already exhibited, and we have found them to be interesting only in the limits already discussed.

What we have found interesting are plots of $N(0)/N(\tau)$ versus τ, where

$$N(\tau) = na^2 \int_0^{R/a} 2\pi\rho\, d\rho \int_0^\infty 4\pi\xi^2 d\xi\, g(\xi, \tau)$$

is the number of particles remaining in the column. Figure 4 shows a series of such plots, for values of $(\lambda_D/a)^2$ ranging from 0.0025 to 10. The plots apparently tend asymptotically to straight lines, for any value of $(\lambda_D/a)^2$. We repeated this for values of a/R ranging from 0.1 to 1 and obtained straight lines in all cases. Of course, we can testify to the linearity only for the duration of the computer run, and numerical considerations limited this to drops in $N(\tau)$ of only a factor of five in some cases. In the limit where $(\lambda_D/a)^2$ is large, the straight lines are associated with our choice of initial distribution. In this limit, one can integrate Eq. (26) to obtain

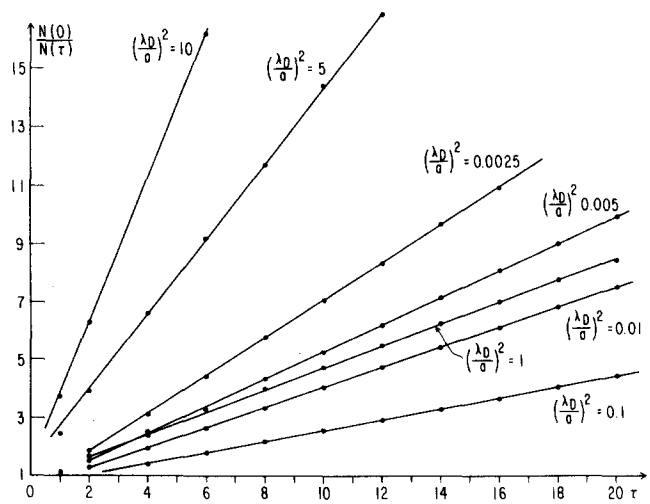

FIG. 4. Number of particles remaining in column as a function of time.

$$\int_0^\infty 4\pi\xi^2 d\xi\, g(\xi,\tau) = \sum_h A_n J_0\left(\rho\frac{a}{R}\chi_{0,n}\right)\int_0^\infty 4\pi\xi^2 d\xi \times \frac{\exp[-\xi^2/2]}{(2\pi)^{3/2}} \exp\left[-\xi^3\frac{\sqrt{\pi}}{8\sqrt{2}}\left(\frac{\lambda_D}{a}\right)^2\left(\frac{a}{R}\right)^2\chi_{0,n}^2\tau\right] . \quad (31)$$

For sufficiently large τ, the second exponential cuts the integral off at small values of ξ, and the Maxwellian may be evaluated at $\xi = 0$. The integral is then proportional to $1/\tau$, so that $N(0)/N(\tau)$ is proportional to τ. This result depends on the assumption that the initial distribution (i.e., the Maxwellian) is non-zero for $\xi = 0$. If the initial distribution were cut off below some particular value of ξ, the density would exhibit exponential decay as a function of τ. In the limit where $(\lambda_D/a)^2$ is small, the straight line result must be independent of the initial distribution. The plasma is heated before significant transport occurs, and the initial distribution is quickly replaced by the Green's function solution to the heating equation [i.e., Eq. (30) evaluated for $\xi' \simeq 0$].

The straight lines should be useful for comparison with experiment. In this regard we note that for large $(\lambda_D/a)^2$ the slope of the lines scale like $(\lambda_D/a)^2$. This is apparent from Eq. (31). Also, in Fig. 4 one can check that the line for $(\lambda_D/a)^2 = 10$ has about twice the slope as the line for $(\lambda_D/a)^2 = 5$. In the limit of small $(\lambda_D/a)^2$, the initial temperature should not matter. However, the scaled time $\tau = t/\tau_m$ is proportional to $\bar{v}$ through the factor $1/\tau_m$. To cancel the $\bar{v}$, the slope must scale as $(a/\lambda_D) \propto 1/\bar{v}$. One can check, in Fig. 4, that the slope for $(\lambda_D/a)^2 = 0.0025$ is about $\sqrt{2}$ times larger than the slope for $(\lambda_D/a)^2 = 0.005$.

The straight lines depend on the assumption that the momentum transfer cross section is constant. For an ambient neutral gas such as krypton, for which the cross section is an increasing function in the relevant energy range, a plot of $N(0)/N(\tau)$ versus τ curves down away from a straight line. Since the electrons gradually cool late in the evolution, they sample a smaller cross section and are transported to the walls more slowly. The opposite effect is observed for the case where the cross section is a decreasing function in the relevant energy range.

Although it is tempting to believe there is a simple general explanation for the straight lines obtained for the case of constant cross section, we have not found such an explanation and are not certain that one exists. As we have seen, the existence of the straight lines depends on the choice of initial distribution, for the case of large $(\lambda_D/a)^2$. Also, the straight lines are sensitive to the details of the velocity dependence in the reduced transport equation, that is, they do not occur for a velocity dependent cross section. Whether or not there is a simple general explanation for the lines, they should be useful for comparison with experiment.[8]

ACKNOWLEDGMENTS

The authors have enjoyed discussions with J. S. deGrassie, C. F. Driscoll, J. H. Malmberg, A. Øien, and W. B. Thompson.

This work was supported by National Science Foundation Grant No. PHY-73-05125 and Energy Research and Development Administration Contract No. E(04-3)-34, Project Agreement No. 85-20.

[1] J. S. DeGrassie, J. H. Malmberg, and M. H. Douglas, Bull. Am. Phys. Soc. 20, 1239 (1975).
[2] P. F. Naccache and M. R. C. McDowell, J. Phys. B: Atom. Mol. Phys. 7, 2203 (1974).
[3] J. H. deGrassie, J. H. Malmberg, and M. H. Douglas, Bull. Am. Phys. Soc. 21, 1115 (1976).
[4] A. Gilardini, *Low Energy Electron Collisions in Gases* (Wiley, New York, 1972).
[5] I. B. Bernstein, in *Advances in Plasma Physics*, edited by A. Simon and W. B. Thompson (Wiley, New York, 1969), Vol. 3, p. 127.
[6] W. B. Thompson, *An Introduction to Plasma Physics* (Addison-Wesley, Reading, Mass., 1962), p. 206.
[7] R. D. Richtmeyer, *Difference Methods for Initial Value Problems* (Wiley, New York, 1967), p. 176.
[8] J. S. deGrassie and J. H. Malmberg (to be published).